Lateral Stress Evolution in Chromium Sulfide Cermets with Varying Excess Chromium

O.E. Petel,[1, a)] G.J. Appleby-Thomas,[2] D.C. Wood,[2] A. Capozzi,[3] A. Nabavi,[3] S. Goroshin,[3] D.L. Frost,[3] and P.J. Hazell[4]

[1)] *Carleton University, Mechanical and Aerospace Engineering, Ottawa, ON, K1S 5B6, Canada*

[2)] *Centre for Defence Engineering, Cranfield University, Defence Academy of the United Kingdom, Shrivenham, Swindon, SN6 8LA, UK*

[3)] *McGill University, Department of Mechanical Engineering, Montréal, QC, H3A 0C3, Canada*

[4)] *School of Engineering and Information Technology, The University of New South Wales, Canberra, ACT 2600, Australia*

(Dated: 12 March 2016)

The shock response of chromium sulfide, a cermet of potential interest as a matrix material for ballistic applications, has been investigated at two molar ratios. Using a combustion synthesis technique allowed for control of the molar ratio of the material, which was investigated under near-stoichiometric (cermet) and excess chromium (interpenetrating composite) conditions, representing chromium:sulfur molar ratios of 1.15:1 and 4:1, respectively. The compacts were investigated via the plate-impact technique, which allowed the material to be loaded under a one-dimensional state of strain. Embedded manganin stress gauges were employed to monitor the temporal evolution of longitudinal and lateral components of stress in both materials. Comparison of these two components has allowed assessment of the variation of material shear strength both with impact pressure/strain-rate and time for the two molar ratio conditions. The dynamic shear strength of the two material systems are comparable to borosilicate and soda-lime glass. The two materials exhibited identical material strength despite variations in their excess chromium contents.

Keywords: Dynamic Material Strength, Cermet, Interpenetrating Composite, Plate Impact

I. INTRODUCTION

Ceramics are a choice material for armour applications due to the combination of their low density, high compressive strength, and hardness, material properties that enable projectile defeat[1–3]. The ballistic performance of a ceramic is typically limited by its brittle nature. The compression and subsequent wave dynamics within an impacted ceramic can lead to tensile failure and extensive crack propagation that is detrimental to the ballistic resistance of the armour. Integrating the ceramics into a composite structure involving multilayer laminates[4], metallic backing materials[5], heavy confinement[6], and ceramic pre-stressing[7,8] are some strategies that have been shown to increase the ballistic performance of a ceramic. The integration of ceramic and metallic components on a finer scale has also been investigated in the form of metal matrix[9–13], cermet[14], and interpenetrating composites (IPC)[15] in an effort to balance the high compressive strength of ceramics with the high fracture toughness of metals to benefit ballistic performance. The present study will evaluate the influence of excess metal content on the dynamic strength of a ceramic-metal system in cermet and interpenetrating metal-matrix composite structures.

A common distinction between a metal matrix composite (MMC) and a cermet is the prominence of the metal or ceramic phases as the continuous medium and their relative proportions. The present investigation will focus on a flame synthesized ceramic, Chromium Sulfide (CrS), that enabled fine control over the proportion of excess metal within its microstructure. CrS can be produced using a combustion synthesis technique known as Self-propagating High-temperature Synthesis (SHS)[16,17], which involves a near-gasless reaction within a melt-cast sulfur and chromium mixture. The product of this reaction is a ceramic with varying amounts of excess chromium integrated into its microstructure, which will depend on the stoichiometry of the green mixture[18]. At the two molar ratios that are investigated in the present study (near-stoichiometric and heavy excess chromium), the microstructure of the system varies from that of a cermet to an interpenetrating composite with metal content closer to that seen in MMCs.

The mechanical properties of the CrS material system have been shown to be highly dependent on the proportion of excess chromium content in its microstructure[19]. Increasing the excess chromium content on a molar ratio basis from 1.15:1 to 4:1 resulted in increases to the Vickers hardness (225 to 305 HV), flexural strength (444 to 727 MPa), Young's modulus (115 to 186 GPa), and fracture toughness (2.36 to 4.12 MPa·m$^{\frac{1}{2}}$). The coincidental increase in strength, hardness, and toughness is desirable for ballistic applications and results in a reduction of the depth of penetration with increasing chromium content while maintaining a constant areal density[20]. An analy-

[a)] oren.petel@carleton.ca

sis of the impacted CrS samples showed evidence of an increase in the ductility of these material systems with increasing chromium content. A thorough study of a titanium carbide-steel cermet demonstrated that the static and dynamic mechanical properties of that cermet was directly related to the microstructure of the steel submatrix[21].

In the present study, we investigate the dynamic material strength of CrS samples in a cermet and IPC composite formulation with two molar ratios using a plate impact technique[22], which has previously been linked to ballistic depth of penetration performance[23]. The dynamic strength of the materials can be determined from the measurement of principal stresses with embedded manganin gauges[24–26]. These types of measurements have been made for a variety of materials ranging from metals[27,28] to ceramics[23,29], elastomers[30,31], and particle suspensions[32]. The present investigation will investigate the influence that a high chromium content has on the dynamic strength of CrS in a cermet and IPC formulation, in light of the published ballistic performance, ductility, and mechanical property variations.

II. EXPERIMENTAL CONFIGURATION

A. Material Preparation

The chromium sulfide (CrS) samples were prepared at two different molar ratios of chromium to sulfur, a near-stoichiometric ratio of 1.15:1 (slight chromium excess) and a ratio of 4:1 (heavy chromium excess). The chromium powder that was used in these studies had a mean particle size of 5 microns and was sourced from Atlantic Equipment Engineers. The sulfur powder was sourced from American Chemicals. Once mixed at the appropriate ratios, the powders were premixed on a roller mill for an hour prior to melting the sulfur in a heating sleeve, which resulted in a thick slurry of liquid sulfur and chromium powder, the green (unreacted) mixture. This slurry was then placed under vacuum while being agitated on a vortex mixer to remove gases trapped by the powders. Following degassing, the green mixture was cast into a preheated mould and allowed to solidify with a nichrome wire embedded within it. The samples were then placed in a reaction chamber that was pressurized with Argon to 275 bar, at which point the nichrome wire was used to ignite the mixture.

The initiated reaction that propagates through the mixture was highly exothermic and nearly gasless. Although the equilibrium calculations show the combustion reaction as a solid-solid process, there is some gas production that results in final product porosity, which can be inhibited by igniting the green mixture in a high-pressure inert atmosphere. The final product of the combustion process is solid CrS interspersed within discrete chromium regions[17,18]. Due to the elevated adiabatic flame temperatures of the reaction, care must also be taken to reduce the thermal stresses on the material during cooling that may lead to internal cracking of the final product. Reducing the prevalence of these thermal cracks was managed by introducing directional cooling of the samples. A thorough discussion of the synthesis process was given by Nabavi et al.[18,19]. The measured densities of the 1.15:1 and 4:1 molar ratio Cr:S samples were approximately 3.88 ± 0.1 g/cm^3 (97% of theoretical maximum density) and 5.08 ± 0.1 g/cm^3 (93% of theoretical maximum density), respectively. Analysing the phase diagram of Cr-S[33] predicts that the cermet has a Pyrrhotite phase with the formula $Cr_{1-x}S$ with (x between 0 and 0.2), which is consistent with an XRD analysis of the cermet[18].

A photograph of the bulk CrS samples and a set of backscatter images of the samples are shown in Fig. 1. These images show that the near-stoichiometric sample is a cermet, primarily ceramic with some interspersed metal inclusions, while the sample with heavy chromium excess is a CrS-Cr IPC with metal-ceramic ratios that are more consistent with an MMC. The image in Fig. 1b demonstrates that the cermet sample had a reasonably uniform microstructure, although small discrete excess chromium and void regions are visible. In contrast, the CrS-Cr IPC samples with heavy chromium excess (seen in Fig. 1c) show large discrete chromium regions surrounded by continuous interstitial CrS regions. The majority of these chromium regions are significantly larger than the initial mean particle size of the chromium powder used in the synthesis.

B. Mechanical Properties of the Samples

A preliminary characterization of these materials involved measuring their longitudinal sound speed and Poisson's ratio. The longitudinal sound speeds of the CrS cermet and IPC were measured with a Panametrics 5077PR pulse-receiver unit (Olympus) using 5 MHz transducers in a pulse-echo configuration and were measured to be 4240 m/s and 4940 m/s, respectively. The Poisson's ratio was determined from a combination of nanoindentation and fracture toughness measurements. The Poisson's ratio of the materials are required to define the elastic responses of the materials, particularly predicting the dynamic compressive strength that could be expected.

A nanoindenter (Hysitron TI 950 Triboindenter) with a diamond Berkovich tip[34] was used to determine the Vickers hardness of the sample. Combining this measured Vickers hardness with the Young's modulus determined previously from fracture toughness testing[19], and an analysis technique described by Zorzi and Perottoni[35], an estimate of the Poisson's ratio could be made. The expression relating these values to the Poisson's ratio is

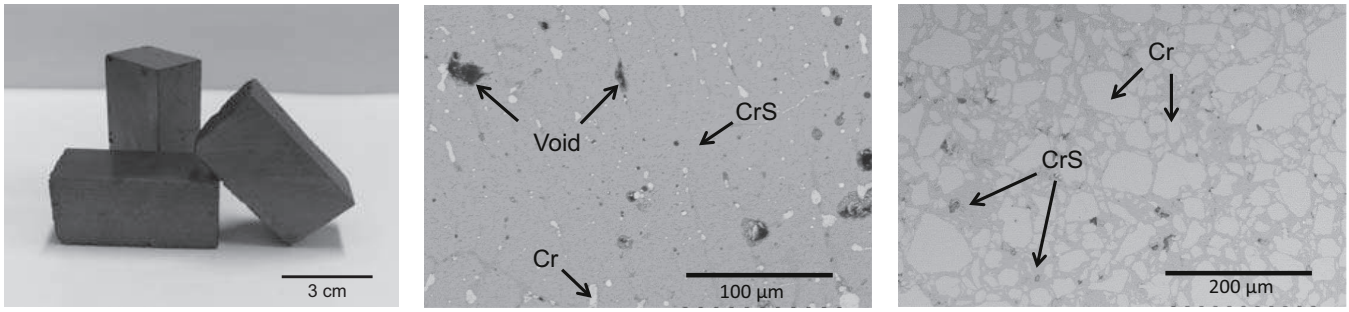

FIG. 1. (a) A photograph of CrS samples. Backscatter images of the CrS samples at a molar ratio of (b) 1.15:1 Chromium:Sulfur and (c) 4:1 Chromium:Sulfur. The backscatter images were adapted from Nabavi et al.[19]

given as

$$H_v = 2\left[\frac{9E}{8}\frac{(1-2\nu)^2}{(1+\nu)^3}\right]^{0.585} - 3, \qquad (1)$$

where H_v is the Vickers hardness. An average of 10 nano-indentation measurements of the CrS cermet resulted in a Vickers hardness and Poisson's ratio of of 4.97 GPa and 0.29, respectively. This value of Vickers hardness is larger than the hardness measured previously for the same samples[19], which is likely due to the size of the indentation tip with respect to the scale of porosity having influenced the previous results.

Given the microstructure of the IPC, with regions of chromium that are large in comparison to the indentation tip size, it was determined that nano-indentation would not provide meaningful results for the IPC. Therefore, to obtain a reasonable estimate of the Poisson's ratio for the IPC, a volume-weighted mixture model was used to estimate the Poisson's ratio of the IPC[36]. The resulting Poisson's ratio was found to be 0.25 for the IPC, which is close to the excepted value for Chromium of 0.21[37]. The values of the Poisson's ratio determined from the nano-indentation of the sample are close to the expected values for these materials and will be used for comparison to the plate impact data.

C. Plate Impact Configuration

A plate impact experiment is a standard technique to investigate the dynamic response of a material at high strain rate under a uniaxial strain loading[22]. The impact experiments were carried out with the 50-mm internal bore single-stage gas gun located at Cranfield University. Three flyer plate types were used in the present study, a 10 mm thick aluminum plate, a 10 mm thick copper plate, and a 5 mm copper plate over a velocity range of 316 to 877 m/s. Using the three different impactor configurations allowed for a broader range of stress states to be achieved for the investigations, given the velocity constraints of the gas gun. The two schematics in Fig. 2 show the gas gun muzzle and diagnostic configuration within the test sample, respectively. The focus of the experimental work was to evaluate the evolution of the stresses within the CrS samples at different molar ratios, so the integration of the manganin gauges was of particular importance.

Each sample of CrS was cut to 25 x 25 x 60 mm and inspected for excessive porosity or cracking. Suitable samples were then polished to ensure sufficiently perpendicular surfaces to enable accurate manganin gauge placement. Two manganin gauges were placed within the target to measure the longitudinal and lateral stresses within the CrS sample as a result of the plate impact. The longitudinal manganin gauge was placed between the cover plate (matched to the flyer plate material) and the CrS in a Mylar encasement similar to the configuration described by Millett et al.[26]. A low-viscosity, epoxy resin was used in the gauge package to adhere the manganin gauges to the insulating Mylar layers. There has been some contention as to the interpretation of the lateral principal stress measurements due to the packaging of the manganin gauge[38,39], however a careful examination of published data shows similar results obtained across methodologies[40]. The longitudinal gauges were calibrated according to the method described by Rosenberg et al.[24]. The lateral manganin gauge was placed 4 mm from the impact face of the CrS samples in the center of the impact plane, similarly contained within a Mylar and epoxy encasement[26]. The calibration of the lateral manganin gauge followed the method initially described by Rosenberg et al.[25,41]. The results will be presented with a time-shifted axis to allow a direct comparison of the evolution of the two stresses, and thus the deviatoric stress component, within the impacted sample. The manganin gauges were sourced from Vishay Micro-Measurements and were of type LM-SS-125CH-048 and J2M-SS-580SF-025 for the longitudinal and lateral stress measurements, respectively.

TABLE I. Material Properties for the CrS Cermet and IPC samples

Material	Chromium Volume Fraction	CrS Volume Fraction	ν
Chromium	1.000	0.000	0.21[37]
Cermet	0.056	0.954	0.29
IPC	0.507	0.493	0.25

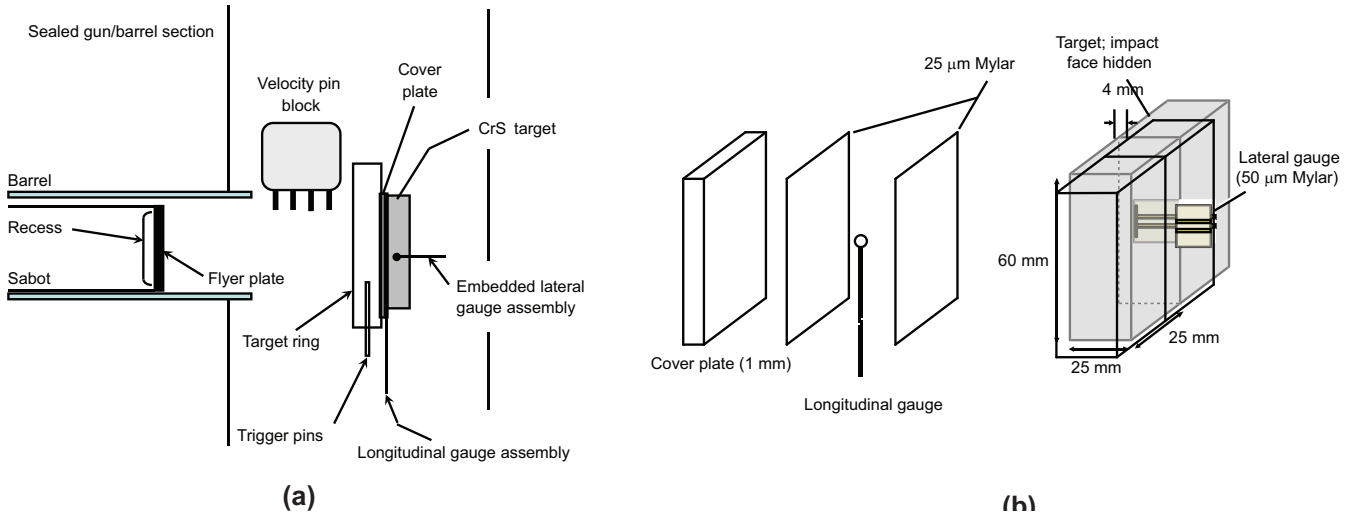

FIG. 2. Schematics of (a) the experimental gas gun assembly and (b) the sample configuration, illustrating the placement of the diagnostic gauges.

III. EXPERIMENTAL RESULTS

Four samples of each type were tested in the present series of experiments. The wave velocity-particle velocity relationships (U_S-u_P) for the materials were determined from the transit times between the longitudinal and lateral manganin gauge and knowledge of the flyer plate velocities. The inflection point of the rise in the manganin gauge signal was taken as the arrival time of the wave. The U_S-u_P data for both the cermet and IPC are plotted in Fig. 3. The trend of the data for the cermet demonstrates the same bilinear Hugoniot trend seen in previous studies of shock wave propagation through a tungsten carbide-cobalt cermet[42]. It was suggested by those authors that the bilinear nature of that data could be explained by a diffuse elastic limit in the material, whereby the cermet has reached its elastic limit while the tungsten carbide particles remained elastic. In the present data, the microstructure of the CrS cermet is dissimilar to that of the tungsten carbide-cobalt cermet, meaning that the diffuse elastic limit explanation is not directly relevant. It is more likely that the materials are being loaded in their elastic-plastic wave regime, although the gauges were not able to confirm the presence of an elastic precursor wave with any degree of certainty.

The longitudinal and lateral stress histories within the 1.15:1 molar ratio, near-stoichiometric, CrS cermet samples under the various impact conditions are shown in

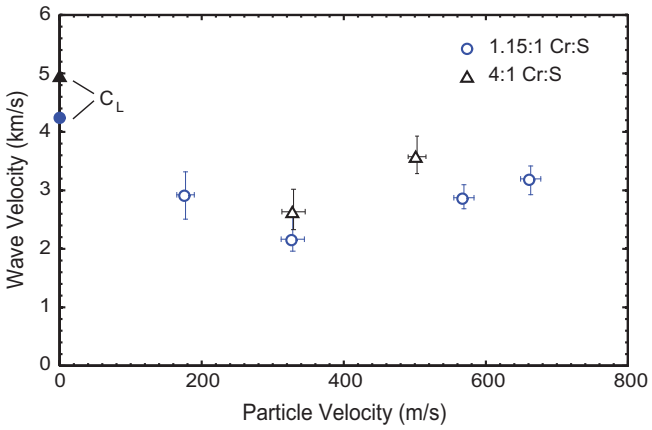

FIG. 3. U_S-u_P data for the cermet and IPC. Longitudinal sound speeds for the two sample types are shown as filled markers.

Fig. 4a and Fig. 4b, respectively. Recall that the lateral gauge is recessed by 4 mm, however the signals have had their time axis translated for comparison purposes. The time axis for the lateral manganin gauge has been shifted with respect to its offset and the measured wave speed. There are several features in the stress histories that are worth noting, particularly in the lateral stress signals (Fig. 4b), which possess a multi-stage rise. This

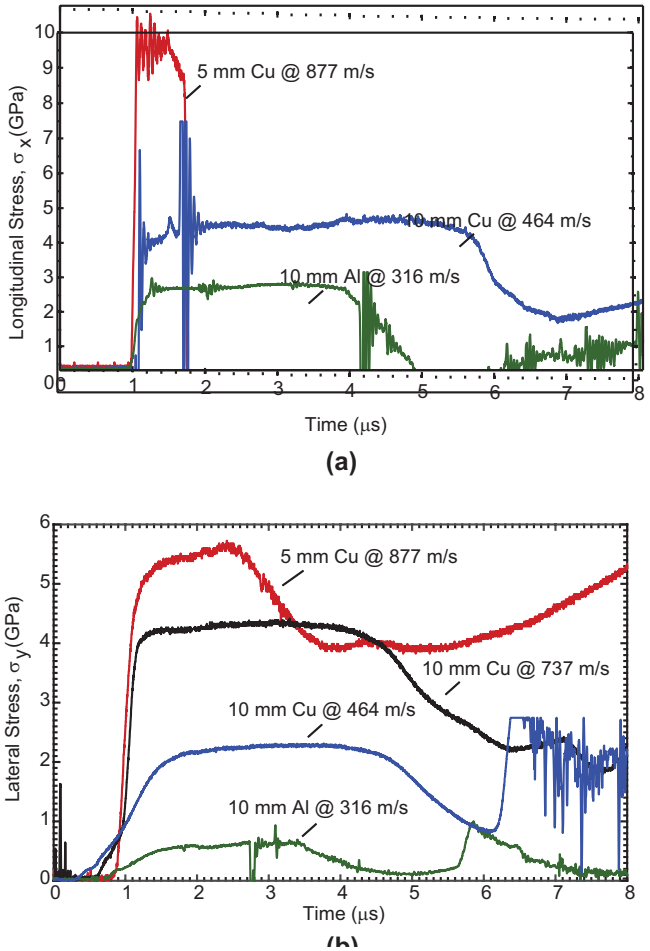

FIG. 4. The experimental stress histories within the near-stoichiometric (1.15:1 molar ratio) CrS for several impact conditions measured with (a) a longitudinal manganin gauge and (b) a lateral manganin gauge. The time bases of the traces have been normalized for comparison purposes.

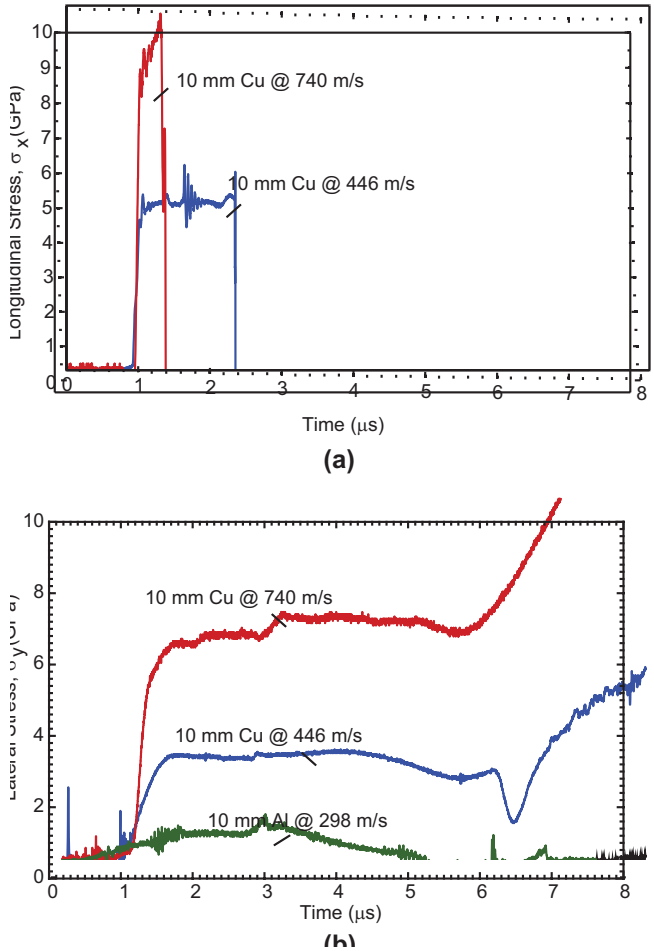

FIG. 5. The experimental stress histories within the heavy chromium excess (4:1 molar ratio) CrS for several impact conditions measured with (a) a longitudinal manganin gauge and (b) a lateral manganin gauge. The time bases of the traces have been normalized for comparison purposes.

response may be indicative of an elastic precursor in the material under the impact conditions; however, the rate-dependency of the lateral stress history, the effects of the manganin gauge encasement, and the level of porosity in these samples make it difficult to draw a firm conclusion with regards to a Hugoniot elastic limit. The shock Hugoniot data would suggest that material response is elastic-plastic in this range of impact conditions. It is worth emphasizing that the complexity of lateral gauge interpretation, given the inherent rise times of the signals, makes the detection of such features difficult[26,43–45].

The longitudinal and lateral stress histories within the 4:1 molar ratio IPC samples with heavy chromium excess under the various impact conditions are shown in Fig. 5a and Fig. 5b, respectively. The general trends of the stresses that were measured within these samples were similar to those observed for the near-stoichiometric CrS cermet. As a result of the higher density and sound speed recorded in the IPC, it was expected that the stress levels would be higher, as seen experimentally. A common feature of the lateral manganin gauge measurements in both samples is a stress increase approximately 5 μs after the primary wave arrives. Based on the configuration of the experiment and wave speeds in the materials, these features are associate with the arrival of lateral expansion at the gauge location rather than a meaningful material response to the impact.

The primary interest of the present study was to determine the dynamic material strength of both CrS samples. The deviatoric component of stress within a material can be determined from measurements of the principal stresses using the expression,

$$\tau = \frac{\sigma_{long} - \sigma_{lat}}{2} \tag{2}$$

where τ is the deviatoric stress in the material and σ_{long} and σ_{lat} are the longitudinal and lateral principal stresses

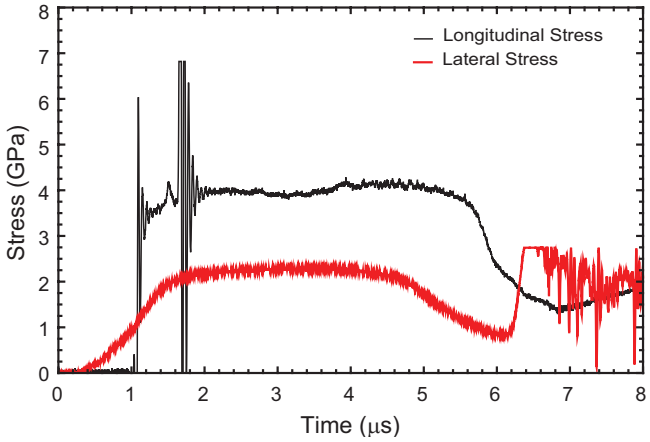

FIG. 6. A plot of the longitudinal and lateral stress histories within the near-stoichiometric CrS cermet sample for a 10-mm copper plate impact at a velocity of 464 m/s.

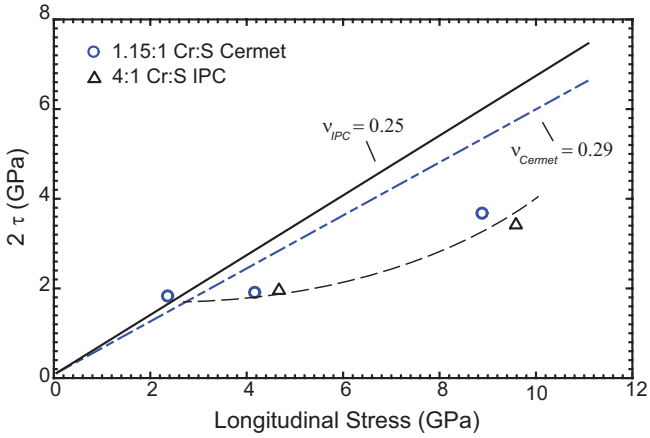

FIG. 7. Variation of the deviatoric stress with longitudinal stress for the CrS cermet and IPC.

in the material, respectively. The relationship between the two principal stresses and their evolution within the sample is shown for a single experiment (464 m/s impact velocity) involving the CrS cermet in Fig. 6. The stress history shows a stable stress region in both signals through several microseconds with some evidence of slight softening. At later times, the increase in deviatoric stress may be due to the configuration of the experiment with respect to the arrival of the effects of lateral expansion of the sample. The magnitude of the principal stresses used in calculating the deviatoric component are taken from those constant stress regions.

The deviatoric stresses of the impacted samples for which both gauges provided sufficiently long signals are summarized in Fig. 7. If we examine the data for the CrS cermet sample, the two lower stress experiments show identical deviatoric stresses, despite the difference in their longitudinal stresses. The higher impact stress investigated resulted in a larger deviatoric stress. The lateral gauge signal from this experiment shows slight softening of the material. Perhaps the softening of the deviatoric stress component at this higher impact stress would be indicative of a failure front passing through the cermet resulting in a constant plastic flow stress, however further investigation of the materials is required to confirm this behaviour.

The deviatoric stresses measured in the experiments involving the heavy chromium excess IPC samples are shown in Fig. 7. The deviatoric stress levels for the IPC are quite similar to the values measured for the cermet. The similarity of the features and deviatoric stress levels suggest that the dynamic response of both materials is likely related to a specific response of the CrS phase itself to the high-strain-rate loading. Given the difference in the microstructures of the two materials, their static material properties[19], Poisson's ratios, and the previous ballistic experimental results showing the influence of the chromium addition on the failure response[20], this result was unexpected.

IV. DISCUSSION

The CrS cermet and IPC that were investigated in the present study had a markedly different microstructure, although both had a continuous CrS phase. The near-stoichiometric cermet was primarily a solid CrS bulk structure with a spattering of small dispersed chromium pockets. In contrast, the IPC with a heavy chromium excess showed a continuous interstitial CrS phase that weaves its way through a dominant network of large chromium regions, although their volume fractions are quite similar (Table I). The expectation would be that the evolution of the stress histories in these two materials would be considerably different, particularly the deviatoric response due to the expected relative contributions from the CrS and chromium.

A common representation of deviatoric stress data is to plot its trend as a function of the impact (longitudinal) stress. Fig. 7 shows the relationship between the longitudinal stress and twice the deviatoric stress for the cermet and IPC, calculated according to equation 2. For an elastic material, these terms should follow a single trendline until the Hugoniot elastic limit is reached. The data points are taken from the stress plateaus seen in the longitudinal and lateral manganin gauge data plotted in Figs. 4 and 5. The analytical relationship between longitudinal and deviatoric stresses for an elastic material is mediated by the Poisson's ratio of the material, as described by the expression

$$2\tau = \frac{1-2\nu}{1-\nu}\sigma_x. \tag{3}$$

Using equation (3) along with the Poisson's ratio measurements, the predicted elastic responses of the shear

strength to longitudinal stress relationship for the CrS cermet and IPC are shown in Fig. 7 for comparison to the data. In Fig. 7, one notices that the measured shear strength in the materials is approximately constant for the CrS Cermet despite a doubling of the impact stress. This response is inconsistent with an elastic material response and we can therefore conclude that the sample is being loaded beyond its respective Hugoniot elastic limit. In Fig. 7, there is a marked deviation of the measured material strength from the expected elastic response of the materials. The common interpretation of similar trends in ceramics is that the deviation relates to the post-failure dynamic response of the material[46]. Fig. 7 shows a classic loss of strength among the cermet and IPC in the failed region. A trendline has been drawn through the data points in Fig. 7 to illustrate the intersection of the data with the predicted elastic response. The intersection of these two lines identifies an Hugoniot elastic limit of approximately 2.9 GPa and 2.6 GPa for the cermet and IPC respectively. The deviatoric stresses for both the CrS cermet and IPC samples follow a similar trendline, demonstrating that the shear strength of the materials at their elastic limit is nearly identical. The shear strength of the materials remain similar well into their plastic response, although from the limited data set, it appears that the cermet retains a marginally higher shear strength at the highest impact stresses investigated. The post-failure material strengths and Hugoniot elastic limits of the cermet and IPC investigated are consistent with data collected for tungsten carbide cobalt cermet at the lower impact stresses[42]. Significant differences between the response of the these materials are evident at higher impact stresses, where the material strength of the cemented tungsten carbide cermet is twice that of the CrS-based materials and is considerably close to its expected elastic response. In both CrS-based materials, there appears to be a slight dependence of the dynamic strength on longitudinal stress in the failed region.

Based on the similarity of the dynamic strength of both materials, which was surprisingly similar, it appears that the dynamic strength response of both materials is dominated by the CrS itself, with little discernible influence from the presence of excess chromium. This result was unexpected for several reasons. Firstly, the Poisson's ratio and elastic prediction for the materials would suggest that the IPC should show a larger deviatoric stress response, however this was not seen experimentally. Secondly, quasi-static material property measurements for these two materials such as the fracture toughness, Young's modulus and Vickers hardness would suggest that the addition of excess chromium to the cermet results in a significant strengthening of the material[19], however this is not seen under dynamic loading. In contrast, the addition of excess chromium seems to have lowered the Hugoniot elastic limit slightly and possibly reduced the strength of the material at increasing impact stresses.

Examining the microstructure of the cermet and IPC (Fig. 1), CrS is the only continuous material common to both samples, as the chromium regions are discretely distributed within the cermet. The addition of chromium does provide some level of increased plasticity within the samples, which was shown to be beneficial under ballistic loading[20], however there is relatively no influence of the chromium to the dynamic strength of the material, as seen in the present study. Despite the expected influence of the excess chromium regions on the dynamic strength, the results indicate that the interconnected CrS regions dominate the strength of the samples at these elevated strain rates. A similar material response was observed by Klein et al.[21] in a study on the effect of heat treatment on an IPC cermet (titanium carbide-steel) on the dynamic material properties of the material, which was dominated by the properties of a single component based on the heat treatment applied. In the present study, the material composition of the IPC was not varied, however the similarity of the dynamic properties of the IPC and CrS Cermet, despite the excess chromium present at approximately 50% by volume in the IPC microstructure.

V. CONCLUSIONS

A set of CrS samples with varying metal content, which are materials of possible interest as a matrix in an MMC type armour configuration, have been investigated using plate impact loading to determine their dynamic shear strength at relevant loading conditions. The dynamic shear strengths of the two materials (a CrS cermet and CrS-Cr IPC) were measured to be quite similar to that of borosilicate and soda-lime glass. Despite the variation of quasi-static material properties based on excess chromium content, the present experimental results showed that the excess chromium content did not have any significant effect on the dynamic shear strength of the materials. The present results demonstrate that further investigation into the effect of material proportions on the dynamic strength of multi-component materials is warranted.

ACKNOWLEDGMENTS

The authors thank Andrew Roberts for his assistance in conducting the experiments in the present study. The authors appreciate Andrew Higgins for his input regarding the synthesis of the Chromium Sulfide samples. This work was conducted with the financial support of the Natural Sciences and Engineering Research Council of Canada under a strategic partnership grant. OE Petel would like to acknowledge funding support from the Natural Science and Engineering Research Council of Canada Discovery Grant program.

[1] M. Wilkins, C. Honodel, and D. Sawle, *An approach to the study of light armor* (Lawrence Livermore National Laboratory Report UCRL-50284, 1967).

[2]Z. Rosenberg and Y. Yeshurun, International Journal of Solids and Structures **7**, 357 (1988).
[3]D. Shockey, A. Marchand, S. Skaggs, G. Cort, M. Burkett, and R. Parker, International Journal of Impact Engineering **9**, 263 (1990).
[4]S. Yadav and G. Ravichandran, International Journal of Impact Engineering **28**, 557574 (2003).
[5]M. L. Wilkins, International Journal of Engineering Science **16**, 793 (1978).
[6]H. Espinosa, N. Brar, G. Yuan, Y. Xu, and V. Arrieta, International Journal of Solids and Structures **37**, 4893 (2000).
[7]C. Han and C. T. Sun, International Journal of Impact Engineering **24**, 597 (2000).
[8]T. J. Holmquist and G. R. Johnson, International Journal of Impact Engineering **31**, 113 (2005).
[9]S. J. Bless, D. L. Jurick, S. P. Timothy, and M. A. Reynolds, in *Shock-Wave and High Strain Rate Phenomena in Materials*, edited by M. A. Meyers, L. E. Murr, and K. P. Staudhammer (Marcel Dekker, 1992) pp. 1051–1058.
[10]R. Vaziri, D. Delfosse, G. Pageau, and A. Poursartip, International Journal of Impact Engineering **13**, 329 (1993).
[11]Y. Gu and V. F. Nesterenko, Journal of Composite Materials **41**, 2313 (2007).
[12]I. A. Ibrahim, F. A. Mohamed, and E. J. Lavernia, Journal of Materials Science **26**, 1137 (1991).
[13]H. Wadley, M. OMasta, K. Dharmasena, B. Compton, E. Gamble, and F. Zok, International Journal of Impact Engineering **62**, 99 (2013).
[14]B. G. Compton and F. W. Zok, International Journal of Impact Engineering **62**, 75 (2013).
[15]H. Chang, J. Binner, R. Higginson, P. Myers, P. Webb, and G. King, Materials Science and Engineering: A **528**, 2239 (2011).
[16]A. G. Merzhanov, Combustion Science and Technology **98**, 307 (1994).
[17]S. Goroshin, A. Miera, D. L. Frost, and J. H. S. Lee, Symposium (International) on Combustion **26**, 1883 (1996).
[18]A. Nabavi, A. Capozzi, S. Goroshin, D. Frost, and F. Barthelat, Journal of Materials Science **49**, 8095 (2014).
[19]A. Nabavi, S. Goroshin, D. Frost, and F. Barthelat, Journal of Materials Science **50**, 3434 (2015).
[20]J. Loiseau, A. Nabavi, A. Capozzi, O. E. Petel, S. Goroshin, F. Barthelat, D. L. Frost, and A. J. Higgins, Journal of Dynamic Behaviour of Materials **1**, 347 (2015).
[21]B. Klein, N. Frage, M. P. Dariel, and E. Zaretsky, Journal of Applied Physics **93**, 968 (2003).
[22]M. A. Meyers, *Dynamic behavior of materials* (John Wiley & Sons, 1994).
[23]N. K. Bourne, International Journal of Impact Engineering **35**, 674683 (2008).
[24]Z. Rosenberg and Y. Yaziv, D.and Partom, Journal of Applied Physics **51**, 3702 (1980).
[25]Z. Rosenberg and Y. Partom, Journal of Applied Physics **58**, 3072 (1985).
[26]J. C. F. Millett, N. K. Bourne, and Z. Rosenberg, Journal of Physics D: Applied Physics **29**, 2466 (1996).
[27]J. C. F. Millett, N. K. Bourne, and Z. Rosenberg, Journal of Applied Physics **81**, 2579 (1997).
[28]G. Appleby-Thomas and P. J. Hazell, Journal of Applied Physics **107**, 123508 (2010).
[29]N. Bourne, J. Millett, Z. Rosenberg, and N. Murray, Journal of the Mechanics and Physics of Solids **46**, 1887 (1998).
[30]N. K. Bourne and J. C. F. Millett, Proceedings of the Royal Society of London A: Mathematical, Physical and Engineering Sciences **459**, 567 (2003).
[31]J. C. F. Millett, G. Whiteman, S. M. Stirk, and N. K. Bourne, Journal of Physics D: Applied Physics **44**, 185403 (2011).
[32]O. E. Petel and A. J. Higgins, Journal of Applied Physics **108**, 114918 (2010).
[33]P. Waldner and W. Sitte, International Journal of Materials Research **102**, 1216 (2011).
[34]W. C. Oliver and G. M. Pharr, Journal of Materials Research **7**, 1564 (1992).
[35]J. Zorzi and C. Perottoni, Materials Science and Engineering: A **574**, 25 (2013).
[36]M. W. Hyer, *Stress analysis of fiber-reinforced composite materials* (DEStech Publications, 2009).
[37]H. Gercek, International Journal of Rock Mechanics & Mining Sciences **44**, 1 (2007).
[38]R. E. Winter, G. D. Owen, and E. J. Harris, Journal of Physics D: Applied Physics **41**, 202006 (2008).
[39]R. E. Winter and E. J. Harris, Journal of Physics D: Applied Physics **41**, 035503 (2008).
[40]J. C. F. Millett, G. Whiteman, N. T. Park, S. Case, and N. K. Bourne, Journal of Applied Physics **113**, 233502 (2013).
[41]Z. Rosenberg, N. K. Bourne, and J. C. F. Millett, Measurement Science and Technology **18**, 1843 (2007).
[42]G. J. Appleby-Thomas, P. J. Hazell, C. Stennett, G. Cooper, K. Helaar, and A. M. Diederen, Journal of Applied Physics **105**, 064916 (2009).
[43]Z. Rosenberg and N. S. Brar, Journal of Applied Physics **77**, 1443 (1995).
[44]Z. Rosenberg and Y. Partom, Journal of Applied Physics **57**, 5084 (1985).
[45]J. C. F. Millett, N. K. Bourne, S. M. Stirk, and G. T. G. III, AIP Proceedings **1195**, 957 (2009).
[46]N. K. Bourne, J. C. F. Millett, and J. E. Field, Proceedings of the Royal Society of London A: Mathematical, Physical and Engineering Sciences **455**, 1275 (1999).